

# Mortality prediction of rats in acute hemorrhagic shock using various machine learning techniques

Joon Yul Choi

Department of Medical Science  
The Graduate School, Yonsei University

Mortality prediction of rats in acute  
hemorrhagic shock using various  
machine learning techniques

Directed by Professor Deok Won Kim

The Master's Thesis  
submitted to the Department of Medical Science  
the Graduate School of Yonsei University  
in partial fulfillment of the requirements for the degree  
of Master of Medical Science

Joon Yul Choi

December 2012

This certifies that the Master's Thesis of  
Joon Yul Choi is approved.

-----  
Thesis Supervisor : Deok Won Kim

-----  
Thesis Committee Member#1 : Incheol Park

-----  
Thesis Committee Member#2 : Boyoung Joung

The Graduate School  
Yonsei University

December 2012

## ACKNOWLEDGEMENTS

의학공학이란 매력적인 학문에 빠져들어 연구가 즐거워 실험을 하다 보니 2년이란 시간이 흘렀습니다. 처음에는 막연히 하고 싶다는, 새로 접한 의학공학이란 학문을 잘 해 낼 수 있을지 걱정이 많았습니다. 그러나, 저를 때론 엄하시게 때론 자비로우시게 학문적으로 또는 인성적으로 올바르게 이끌어 주신 김덕원 교수님께 가장 먼저 감사 드립니다. 출혈성 쇼크라는 의학적 주제로 연구를 시작하여 임상적으로 더 나은 방향을 제시해 주신 박인철 교수님과 정보영 교수님께 감사 드립니다. 신경생물학 수업을 계기로 생리학뿐만 아니라 신경에 대한 관심을 이끌어 주시고, 웃으시며 아낌없이 도움을 주신 남택상 교수님께 감사 드립니다.

처음 연구실에 들어와 생활에 미숙하여 어려움이 있었지만, 많은 도움을 주신 저의 연구실 식구이자 선배이신 경환, 재림, 민경 선배에게 감사합니다. 저에겐 형님들이며 후배인 성권, 정모, 수범 형에게도 좋은 추억 만들며, 연구실 생활 즐겁게 할 수 있게 도움을 줘서 고맙습니다. 문제에 봉착했을 때, 슈퍼맨처럼 문득 나타나 도움을 준 완형이 형에게도 감사합니다. 저의 보물 서회를 연결시켜주고, 항상 긍정적으로 연구에 도움을 준 친구 태근이에게도 감사합니다. 미국에서 처음 뵈어 저를 위해 항상

기도해주시고 가르침 주시며 한걸음 한걸음 나아갈 수 있도록 도움을 주신 최진봉 전도사님께 감사 드립니다. 철 없는 어릴 때부터 함께 해온 정우, 인영이, 주현이, 홍석이, 지현이게도 감사합니다. 부족한 오빠를 항상 응원해주며 옆에 있어준 내 반쪽 서희에게 감사합니다.

끝으로, 항상 늦은 시간 찾아 봐어도 주무시다가 일어나서 반겨주셨던 친할머니, 아침밥 해주시겠다고 새벽에 일어나서 챙겨주신 외할머니, 저보다 의공학에 대해 더 찾아보시며 공부해주시는 아버지, 아낌없이 베풀어 주시는 저의 단짝이신 어머니, 항상 챙겨주고 학문적, 인생적 선배이며 도움을 준 유열이형에게 감사합니다.

2012년 12월  
최준열 드림

# TABLE OF CONTENTS

Abstract .....	1
I. INTRODUCTION.....	3
II. MATERIALS AND METHODS .....	5
1. Physiological data acquisition.....	5
A. Animal preparation .....	5
B. Physiological data measurement.....	7
(A) Measurement equipments .....	7
(B) Heart rate measurement .....	9
(C) Respiration rate measurement.....	10
(D) Blood pressure measurement.....	10
(E) Temperature measurement .....	11
(F) Lactate concentration measurement .....	11
(G) Perfusion measurement.....	12
C. Experimental protocol.....	13
D. Statistical analysis.....	14
2. Mortality predicting model construction.....	15
A. Machine learning techniques .....	15
(A) Logistic regression (LR).....	15
(B) Artificial neural network (ANN).....	16
(C) Random forest (RF) .....	17
(D) Support vector machine (SVM).....	17
(E) Advantages and disadvantages .....	18
B. Model construction .....	19
(A) Data set .....	19
(B) Variable selection .....	19
(C) Performance evaluation of the mortality predicting models	

.....	21
III. RESULTS .....	23
1. Experimental data resulting from hemorrhage .....	23
A. Experimental data for the survival and death groups .....	23
B. Changes in physiological data during hemorrhage .....	25
C. All measured data at the end of hemorrhage .....	29
D. Correlation coefficients of all measured data with mortality ..	30
2. Variable selection and performance of the mortality predicting models .....	31
A. Logistic regression .....	31
(A) Selected variables in the training set and ROC curve of LR model .....	31
B. Artificial neural network .....	32
(A) Selected variables in the training set .....	32
(B) Performance of the mortality predicting model in the testing set .....	32
C. Random forest .....	34
(A) Selected variables in the training set .....	34
(B) Performance of the mortality predicting model in the testing set .....	34
D. Support vector machine .....	36
(A) Selected variables in the training set .....	36
(B) Performance of the mortality predicting model in the testing set .....	36
3. Optimal mortality predicting model selection for hemorrhagic shock .....	39
IV. DISCUSSION .....	40
V. CONCLUSION .....	46

REFERENCES .....	47
ABSTRACT (IN KOREAN).....	51
PUBLICATION LIST .....	53

## LIST OF FIGURES

Figure 1. Experimental preparation and measurement .....	6
Figure 2. Diagram of measurement system .....	7
Figure 3. Photo of Power Lab 8/30 .....	8
Figure 4. Example of Lab Chart 7 Pro .....	8
Figure 5. Blood lactate analyzer for this study .....	8
Figure 6. Laser Doppler perfusion monitor and Perisoft for Window .....	9
Figure 7. Photo of placement of ECG electrodes.....	9
Figure 8. Photo of respiratory belt around a rat's chest.....	10
Figure 9. Blood pressure sensor used in this study .....	10
Figure 10. Calibration of blood pressure sensor (left) and calibration graph (right) .....	11
Figure 11. Rectal probe for measuring temperature (a=5 cm)	11
Figure 12. Photo of blood sampling from left femoral vein ...	12
Figure 13. Linear interpolation (left) and its equation (right).	12
Figure 14. Perfusion measurement (left) and placement of a probe (right) .....	13
Figure 15. Experimental protocol including measurement of lactate concentration, tail amputation, and period of data analysis .....	14
Figure 16. Algorithm of ANN model .....	16
Figure 17. Algorithm of RF model.....	17

Figure 18. Algorithm of SVM model.....	18
Figure 19. Flowchart of backward elimination variable selection and mortality predicting model construction .....	21
Figure 20. Relative changes in HR, SBP, PPR, and RR during hemorrhage (A), absolute values and relative changes in SI during hemorrhage (B).....	26
Figure 21. Absolute values (left column) and relative changes (right column) in LC, PP, and NI during hemorrhage	28
Figure 22. Receiver operating characteristic curve of LR model.....	31
Figure 23. Receiver operating characteristic curve of ANN model with 3 hidden neurons.....	33
Figure 24. Receiver operating characteristic curve of RF model with 100 trees.....	35
Figure 25. Receiver operating characteristic curve of SVM model using Gaussian kernel function with penalty parameter of 0.1 and scaling factor of 1 .....	38

## LIST OF TABLES

Table 1. Male Sprague - Dawley rat.....	5
Table 2. Advantages and disadvantages of LR, ANN, RF, and SVM .....	18
Table 3. Number of data sets for training and testing sets .....	19
Table 4. Used terminologies for sensitivity, specificity, accuracy in this study.....	22
Table 5. Experimental data for the survival and death groups	24
Table 6. Comparison of all measured data (mean (SD), <i>P</i> ) at the end of hemorrhage between the survival and death groups and AUC data .....	29
Table 7. Correlation coefficients of all variables with mortality .....	30
Table 8. Selected variables and accuracy for ANN models in the training set.....	32
Table 9. Performance of the ANN models with the different number of hidden neurons in the testing set .....	33
Table 10. Selected variables and accuracy for RF models with different number of trees in the training set.....	34
Table 11. Performance of the RF models with different number of trees in the testing set.....	35
Table 12. Selected variables and accuracy for SVM models with the different kernel function in the training set ..	36

Table 13. Performance of the SVM models with the different kernel function in the testing set .....	37
--	----

## ABBREVIATION

ANN: Artificial neural network

ATLS: Advanced Trauma Life Support

AUC: Area under the ROC curve

BP: Blood pressure

DBP: Diastolic blood pressure

ECG: Electrocardiography

HR: Heart rate

LC: Lactate concentration

LR: Logistic regression

MAP: Mean arterial pressure

NI: New severity predicting index

PP: Peripheral perfusion

PPR: Pulse pressure

RF: Random forest

ROC: Receiver operating characteristic

RR: Respiration rate

SBP: Systolic blood pressure

SD: Standard deviation

SI: Shock index

SVM: Support vector machine

TEMP: Temperature

<ABSTRACT>

Mortality prediction of rats in acute hemorrhagic shock using various machine learning techniques

Joon Yul Choi

*Department of Medical Science  
The Graduate School, Yonsei University*

(Directed by Professor Deok Won Kim)

Casualty triage at initial contact on scene by first responders is crucial to save hemorrhagic patients' lives in civilian trauma or on the battlefield. However, there are few studies to demonstrate important physiological variables related to mortality and the most suitable machine learning techniques for casualty triage among various techniques. This study was conducted to suggest a mortality predicting model for casualty triage on scene using various machine learning techniques through a rat model in acute hemorrhage. Furthermore, this study determined important physiological variables for mortality prediction to effectively minimize impression time for first responders.

Thirty-six anesthetized rats were randomized into three groups according to volume of controlled blood loss. Uncontrolled hemorrhage was induced simultaneously by combination of controlled blood loss and tail amputation in all rats. This study measured heart rate (HR), systolic and diastolic blood pressures (SBP and DBP), mean arterial pressure (MAP), pulse pressure (PPR), respiration rate (RR), temperature (TEMP), lactate concentration (LC), peripheral perfusion (PP), shock index (SI,  $SI=HR/SBP$ ), and the new hemorrhage-induced severity index (NI,  $NI=LC/PP$ ) as candidates for input variable of each machine learning techniques. All variables were analyzed for changes between pre- and post-hemorrhage to investigate the effects of hemorrhage on mortality.

The training data set was used to construct models based on popular machine learning techniques including logistic regression (LR), artificial neural networks

(ANN), random forest (RF), and support vector machines (SVM). To select important variables for mortality prediction in a rat model, variables selection was performed with algorithm of consistency subset evaluation using 10-fold cross validation. The testing data set was used to assess the performance of the optimized models consisting of the selected variables for predicting mortality using sensitivity, specificity, accuracy and area under curve (AUC) of the receiver operating characteristic (ROC).

For the LR model, sensitivity, specificity, accuracy, and AUC were 0.678, 1.000, 0.833, and 0.833, respectively. For the ANN model, sensitivity, specificity, accuracy, and AUC were 0.833, 1.000, 0.917, and 0.917, respectively. For the RF model, sensitivity, specificity, accuracy, and AUC were 0.833, 1.000, 0.917, and 0.903, respectively. For the SVM model, sensitivity, specificity, accuracy, and AUC were 1.000, 0.833, 0.917, and 0.972, respectively. The SVM model showed better AUC than that of the LR, ANN, and RF models for mortality prediction. The important variables selected by SVM were LC and NI.

In conclusion, the SVM model with selected variables, LC and NI, was superior to the LR, ANN, and RF models in predicting mortality resulting from acute hemorrhagic shock in a rat model. These machine learning techniques may be very helpful to first responders to accurately make causality triage decisions and rapidly perform proper treatments for hemorrhagic patients in civilian trauma or on the battlefield in the future.

---

Key words: hemorrhagic shock, rat, mortality, new index, shock index, machine learning techniques, support vector machine, random forest

# Mortality prediction of rats in acute hemorrhagic shock using various machine learning techniques

Joon Yul Choi

*Department of Medical Science  
The Graduate School, Yonsei University*

(Directed by Professor Deok Won Kim)

## I. INTRODUCTION

The World Health Organization (WHO) reported that approximately 5 million people died from injury around the world in 2008<sup>1</sup>, and hemorrhagic shock accounts for 30% of these deaths<sup>2</sup>. 33% to 56% of civilian deaths occur during the pre-hospital period, and 80% to 90% of combat deaths occur in far-forward environments<sup>3</sup>. The ability of first responder on scene to prioritize patients and to perform proper treatment has been emphasized in instances of civilian trauma or on the battlefield<sup>4,5</sup>. Hemorrhagic shock is syndrome of circulatory dysfunction causing decreased tissue oxygenation and accumulation of oxygen debt, which ultimately leads to multiple organ system failure if left untreated<sup>6</sup>.

Many studies have evaluated hemorrhagic shock severity using the traditional vital signs, including heart rate (HR), blood pressure (BP), pulse pressure (PPR), and respiration rate (RR), based on The American College of Surgeons' Advanced Trauma Life Support (ATLS) for Doctors. However, use of these traditional vital signs solely has been reported that might be untrustworthy measures due to compensatory mechanisms<sup>6-8</sup>. Recent studies have concentrated on the tissue states to diagnose hemorrhagic shock severity using lactate concentration (LC) and peripheral perfusion (PP)<sup>6,9</sup>. However, Pestel et al.

reported that traditional vital signs were more sensitive in detecting acute hypovolemia than were tissue oxygen tension measurements or regional perfusion, in a swine model<sup>10</sup>.

Shock index (SI), defined as a ratio of HR to systolic blood pressure (SBP), showed better measure of acute blood loss than either HR, SBP, or diastolic blood pressure (DBP) alone<sup>11,12</sup>. Newly proposed hemorrhage-induced severity index (NI), defined as LC/PP ratio, showed a better marker for predicting mortality in rats undergoing acute hemorrhage in comparison to the traditional vital signs, LC, and PP alone as well as SI<sup>13</sup>. However, a computational artificial intelligence model for predicting hemorrhagic shock severity using various physiological variables simultaneously is strongly needed in order to improve similarity to clinical setting and accuracy of diagnosis.

Machine learning is a part of artificial intelligence method using statistical method for data classification<sup>14</sup>. Recently, many studies have applied machine learning techniques to the severity prediction model for hemorrhagic shock. Roberts et al.<sup>15</sup> used a polynomial neural network to predict mortality in hemorrhagic shock using SBP and mean arterial pressure (MAP) in a swine model. Eftekhari et al.<sup>16</sup> compared logistic regression (LR) and artificial neural network (ANN) models for predicting mortality in head trauma patients, and showed ANN significantly outperformed the LR in prediction accuracy. Jang<sup>17</sup> and Choi<sup>18</sup> et al. newly applied support vector machine (SVM) and random forest (RF) classifiers to mortality prediction model using a hemorrhagic rat model. Although each machine learning technique showed possibility to use severity prediction of hemorrhagic shock, a few study considered all the possible physiological variables aforementioned simultaneously for a prediction model and compared which machine learning technique is superior among the techniques popularly used. It will also be expected to select influential variables in predicting hemorrhagic shock mortality for an optimized model in order to minimize triage time for first responders.

In this study, we validated the machine learning techniques with the aim of accurately predicting hemorrhagic shock mortality in a rat model. The

influential variables were also selected among proposed diagnosis indices such as HR, SBP, DBP, MAP, PPR, RR, temperature (TEMP), LC, PP, SI, and NI. Then, the performances of LR, ANN, SVM, and RF models were compared for sensitivity, specificity, accuracy, and area under curve (AUC) of the receiver operating characteristic (ROC).

## II. MATERIALS AND METHODS

### 1. Physiological data acquisition

#### A. Animal preparation

Thirty-six male Sprague-Dawley rats (Orient, Seongnamsi, Korea), 8 to 9 weeks old and weighing 300 to 400 g ( $356 \pm 36$  g), were divided into three groups of 12 rats. These groups were subjected to controlled blood loss of 2.0, 2.5, or 3.0 mL per 100 g animal weight over a 15 min period. The percentages of calculated total blood volume withdrawn from these groups were 32.8%, 41.0%, and 49.2%, respectively (total blood volume [mL] = body weight [g]  $\times$  0.061)<sup>19</sup>. According to ATLS, blood losses of 32.8%, 41.0%, and 49.2% correspond to class III (30% - 40%) and class IV (>40%) hemorrhage<sup>20</sup>. The mean weights of the three groups were not significantly different before blood withdrawal, applying the Kruskal-Wallis test ( $P > 0.05$ ).

Table 1. Male Sprague - Dawley rat

Weight (g)	300-800
Body temperature (°C)	37.5
Heart rate (bpm)	330-480
Blood pressure (mmHg)	Systole: 88-184
	Diastole: 55-145
Blood volume (mL/kg)	60.1
Respiration rate (bpm)	65-110

Rats were anesthetized with an isoflurane inhalation system (RC2; Vet-Equip, Pleasanton, CA, USA); anesthesia was induced with a 5% concentration and maintained with a 2% concentration. Animals were placed in the supine position on the operating table with a heating pad underneath and spontaneously breathed throughout the experiment via an anesthesia cone mask. During the preparation period, rectal TEMP was maintained at 38°C using the heating pad. After incising the right lateral neck and the right and left periphery of the inguinal area, a 24-gauge catheter (Becton Dickinson, Franklin Lakes, NJ, USA) was inserted into the right carotid artery to draw blood, and the catheter was connected to a withdrawal syringe pump (Pump 11 Plus; Harvard Apparatus, South Natick, MA, USA). Another 24-gauge catheter was inserted into the right femoral artery to measure arterial BP, and the catheter was connected to a pressure sensor (1620 Pressure Sensor; MSI Sensors, Hampton, VA, USA). Both catheters were filled with a mixture of heparin sodium (Choongwae Pharmacy Co, Seoul, Korea) and normal saline (500 IU heparin sodium per 500 mL saline). The left inguinal area was made accessible for blood sampling to measure serum LC. All experimental procedures and protocols used in this study were approved by the Institutional Animal Care and Use Committee of Yonsei University Health System, Seoul, Korea.

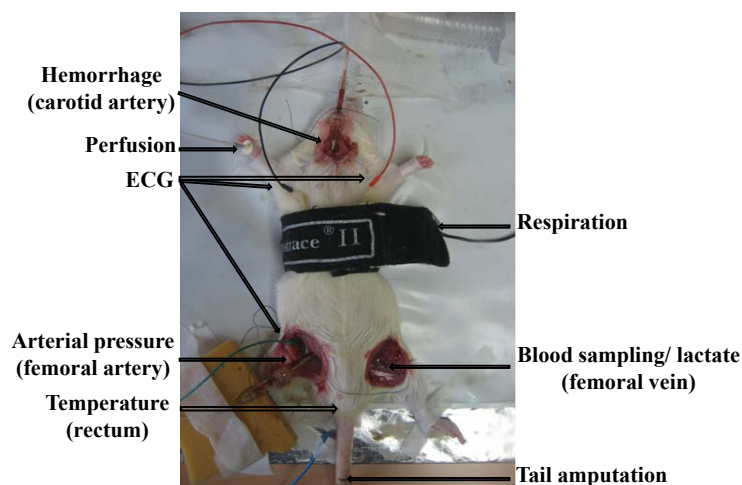


Figure 1. Experimental preparation and measurement

## B. Physiological data measurement

### (A) Measurement equipments

As shown in Figure 2, this study measured physiological variables including HR, SBP, DBP, MAP, PPR, RR, and TEMP with a sampling frequency of 1 kHz using Lab Chart 7 Pro software (AD Instruments, Colorado Springs, CO, USA). The data were fed into an Analog/Digital conversion system (Power Lab 8/30; AD Instruments).

Lactate concentration was measured by a portable blood lactate analyzer (Lactate Pro LT-1710; ARKRAY Inc, Kyoto, Japan) with a detection range of 0.8 to 23.3 mmol/L and a precision of 3%. Approximately 5 $\mu$ L blood samples were needed, and measuring time was 60 s.

Peripheral perfusion was continuously measured using a laser Doppler perfusion monitor (PeriFlux System 5000; Perimed, Stockholm, Sweden) with a probe (Probe 407; Perimed). Perfusion data were acquired with a sampling frequency of 32 Hz and analyzed by computer software (Perisoft for Windows; Perimed).

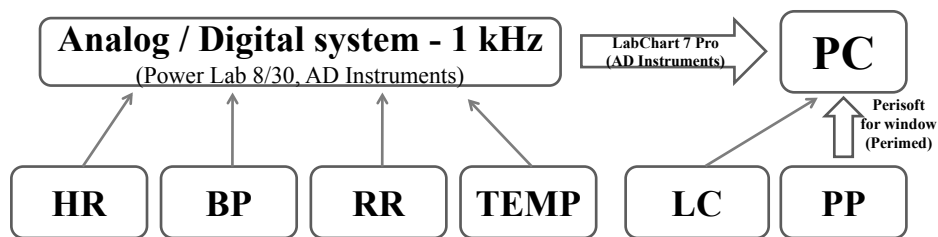


Figure 2. Diagram of measurement system

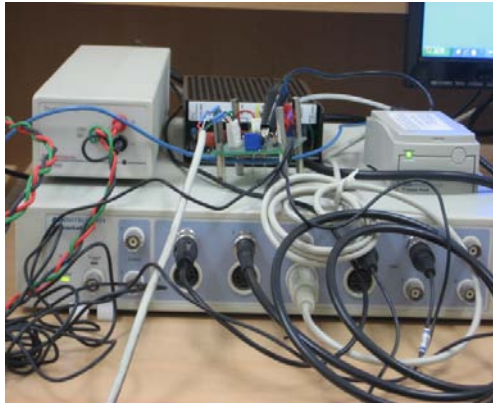


Figure 3. Photo of Power Lab 8/30

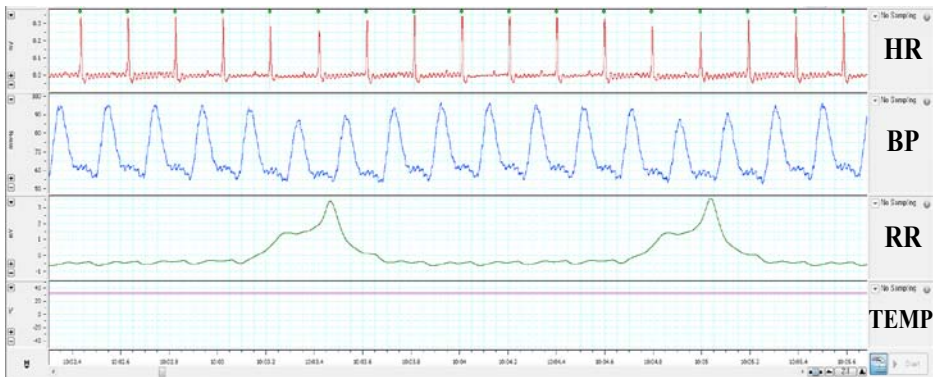


Figure 4. Example of Lab Chart 7 Pro



Figure 5. Blood lactate analyzer for this study

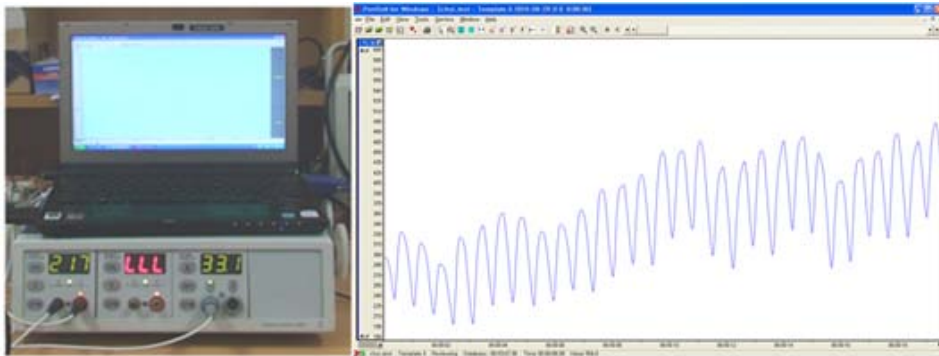


Figure 6. Laser Doppler perfusion monitor and Perisoft for Window

(B) Heart rate measurement

Heart rate was obtained by electrocardiogram signals using three invasive needle electrodes with a biological amplifier (ML136; AD Instruments). The electrodes were inserted in the left and right forelegs and the right hind leg (Figure 7).

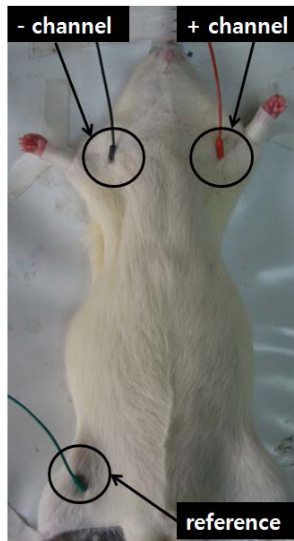


Figure 7. Photo of placement of ECG electrodes

(C) Respiration rate measurement

Respiration was assessed by measuring changes in the thoracic cross-sectional area using a respiratory belt (MLT1132; AD Instruments).

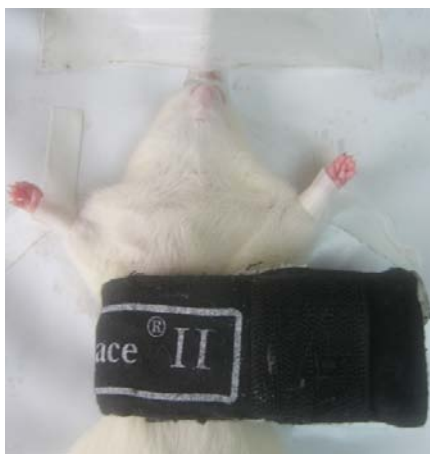


Figure 8. Photo of respiratory belt around a rat's chest

(D) Blood pressure measurement

An invasive BP amplifier was constructed using an instrumentation amplifier (AD620; Analog Device, Norwood, Mass) and the piezo-resistive silicon pressure sensor (Figure 9) that was calibrated with a mercury sphygmomanometer (Figure 10).



Figure 9. Blood pressure sensor used in this study

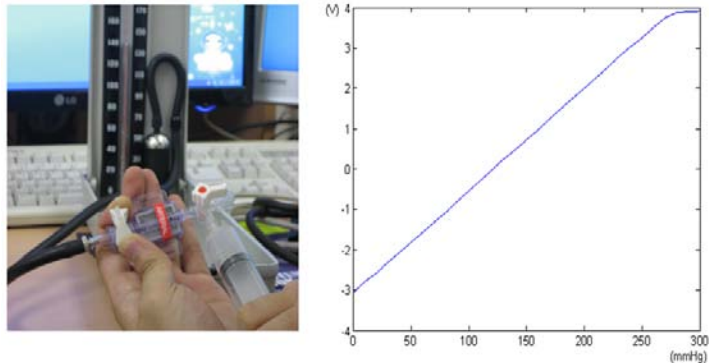


Figure 10. Calibration of blood pressure sensor (left) and calibration graph (right)

#### (E) Temperature measurement

This study measured TEMP in the rats using a rectal probe (MLT1403; AD Instruments), which was inserted approximately 5 cm into the rectum (Figure 11).

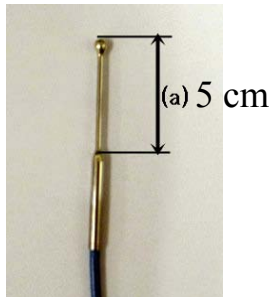


Figure 11. Rectal probe for measuring temperature (a=5 cm)

#### (F) Lactate concentration measurement

Blood sampling for LC was repetitively acquired from the left femoral vein using a 31-gauge insulin syringe (BD Ultra-Fine; Becton Dickinson) as shown in Figure 12. Actual LC values were measured from blood samples taken at

5min intervals from 15 to 45 min, and less frequently from 45 min to the 150min experimental end point. Interim LC values were calculated for every 10s period between blood draws, by linear interpolation using computer software (LabVIEW 2009; National Instruments, Austin, TX, USA)<sup>15</sup>. Linear interpolation was used to calculate the missing data using the gradient between two known points as shown in Figure 13.



Figure 12. Photo of blood sampling from left femoral vein

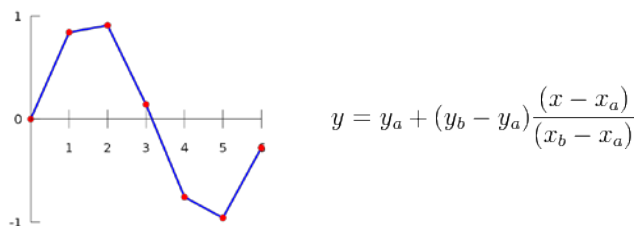


Figure 13. Linear interpolation (left) and its equation (right)

### (G) Perfusion measurement

Peripheral perfusion, defined as peripheral tissue perfusion and skin microcirculation, was continuously monitored by laser Doppler flowmetry with a probe that was attached to the right front sole as shown in Figure 14. The principle of this method is to measure Doppler shift: changes in frequency that light undergoes when reflected by moving objects. A monochromatic laser of 780-nm wavelength from the probe illuminates the skin through an optical fiber, and the light frequency changes when it is reflected by red blood cells 0.5 to 1.0

mm under the skin. This frequency change depends on the blood's local speed. Another receiving optical fiber that is adjacent to the emitting optical fiber collects the backscattered light from the red blood cells and returns it to the monitor. Peripheral perfusion is calculated as the product of the red blood cell concentration and flowing blood speed<sup>21,22</sup>.

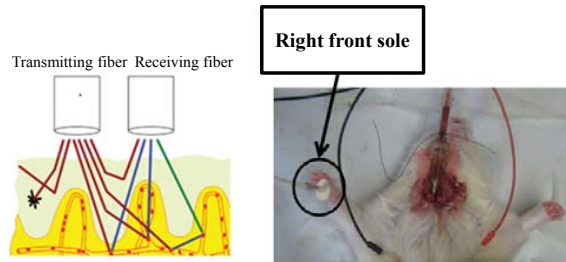


Figure 14. Perfusion measurement (left) and placement of a probe (right)

### C. Experimental protocol

Room TEMP was maintained between 23 °C and 25 °C, and humidity was maintained between 40% and 60% during the experiments. As shown in Figure 15, rats were rested for 15 min before hemorrhage. Volume-controlled hemorrhage was conducted by blood withdrawal from the catheter in the right carotid artery over 15 min (for a total volume of 2.0, 2.5, or 3.0 mL/100 g animal weight). Uncontrolled hemorrhage was performed by tail amputation (75% of its length) 1 min after beginning the volume-controlled hemorrhage. Tail blood was immediately directed into a tube containing heparinized saline, and the blood volume collected was determined by weighing the tube. At 30 min, volume-controlled hemorrhage was ended, and the stump of the tail was tightly bandaged to stop bleeding.

Blood samples for lactate measurement were obtained repeatedly at increments as shown in Figure 15. As severe hypovolemia from hemorrhage is known to be a major causative factor in almost half of hemorrhage-related deaths, especially during the acute period less than 2 h after injury<sup>23</sup>, all data

were collected until death or through 120 min, whichever came first<sup>13,23,24</sup>, to predict mortality at 120 min after hemorrhage cessation. Rats that survived 120 min were killed, and death was defined as the absence of measured MAP<sup>25</sup>.

As all measured data were averaged for every 10 s, six data sets were obtained per minute. To investigate mortality resulting from hemorrhage using all variables, we analyzed data based on the changes between at rest (100%) for 30 s and immediately after the cessation of bleeding for 10 s as shown in Figure 15. The reason for analyzing the short time of 10 s was to limit the effect of hemostasis as much as possible. These data were selected to mimic the scenario where first responders or emergency medical staffs initially encounter bleeding-injured patients with unknown volumes of blood lost to acute hemorrhage, whether it is on the battlefield or in civilian trauma. In these instances, first responders or emergency health care workers must attempt to judge hemorrhagic shock severity by comparing a patient's vital signs with normal values. Shock index and NI was calculated using the measured HR, SBP, LC, or PP values.

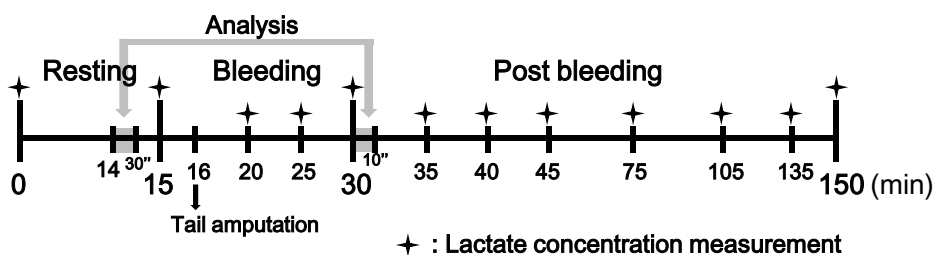


Figure 15. Experimental protocol including measurement of lactate concentration, tail amputation, and period of data analysis

#### D. Statistical analysis

We applied Mann-Whitney U tests to test whether the following variables of weight, HR, SBP, DBP, MAP, PPR, RR, TEMP, LC, PP, SI, and NI in rat groups that either died or survived hemorrhage were significantly different

during a resting period. The relative changes of all variables referenced to pre-hemorrhage were obtained every 1 min for the death and survival groups. All variables for each minute were compared between the survival and death groups using the Mann-Whitney U tests. Receiver operating characteristic curves were generated, and areas under a receiver operating characteristic curves (AUCs) were obtained to determine the optimal variables for predicting mortality among all of the measured variables, using computer software (MATLAB version 2011; Mathworks Inc, Natick, MA).

Correlation coefficient analysis with Spearman rank test was used to evaluate influential variables associated with death resulting from hypovolemia. Strength of the correlation was determined by its correlation coefficient ( $|r| > 0.7$ , strong correlation;  $0.3 < |r| < 0.7$ , moderate correlation;  $0.1 < |r| < 0.3$ , weak correlation;  $|r| < 0.1$  negligible correlation)<sup>26</sup>. All statistical analyses were performed using SPSS 18.0 software (SPSS Inc, Chicago, IL), and  $P < 0.05$  was considered statistically significant.

## 2. Mortality predicting model construction

### A. Machine learning techniques

#### (A) Logistic regression (LR)

Logistic regression is used to generate a predictive model for dichotomous response variables by fitting data to a logistic function (1), which always takes on values between zero and one:

$$P(x) = \frac{1}{1 + e^{-(\alpha + \beta_1 x_1 + \beta_2 x_2 + \beta_3 x_3 + \dots + \beta_d x_d)}} \quad (1)$$

In equation (1),  $\beta_1 \sim \beta_d$  are called the regression coefficients of input variables respectively. Each of the regression coefficients describes the size of the contribution of that risk factor. LR models are usually used for comparison in machine learning studies<sup>14</sup>. We compared the performance of the LR models to that of ANN, RF, and SVM models.

(B) Artificial neural network (ANN)

The basic idea for artificial neural networks is to mimic a biological neural network. In this study, ANN was based on a multi-layer perceptron with feed forward which consisted of three layers: one input, hidden, and output layers as shown in Figure 16. Each layer of the network consisted of a number of elementary processing units called neurons<sup>27</sup>. Artificial neural network with too few hidden neurons would be incapable of differentiating between complex patterns, leading only to a linear estimate of the actual trend. In contrast, if the ANN model had too many hidden neurons, it would follow the noise in the data due to over-fitting, leading to poor generalization for untrained data<sup>28</sup>. Although the optimal number of hidden neurons was determined by empirical method, it has been recently determined depending on the number of input and output variables<sup>25</sup>. This study trained the networks applying between two and ten hidden neurons to obtain the optimal ANN model. The ANN algorithm was based on Levenberg-Marquardt back propagation with epoch of 100 and gradient of less than  $e^{-50}$  to find a predicting solution. Back propagation is an algorithm that finds minimum error changing weight of layers.

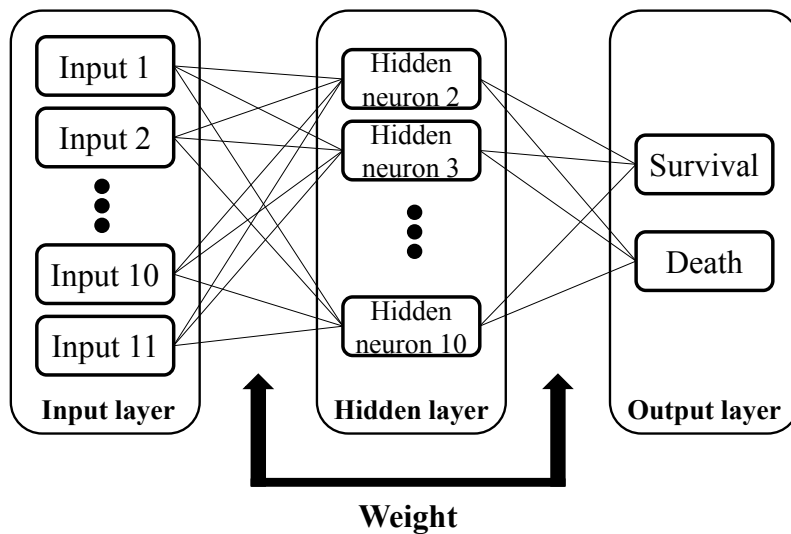


Figure 16. Algorithm of ANN model

(C) Random forest (RF)

Random forest is an ensemble classification algorithm that consists of many decision trees and outputs by independent trees (Figure 17). Input 1 ~ Input 11 are the input variables for Random forest model.  $Data_1 \sim Data_t$  are training data selected randomly from the data sets with input variables to make the decision trees,  $T_1 \sim T_t$  are the decision trees. Each tree is built independently in combination of a bagging idea and random selection of input variables. The result is based on a majority vote of the classification of all trees<sup>14</sup>. Thus, the goal of random forest is to classify accurately by controlling the number of the trees. This study investigated mortality prediction models arbitrarily using trees of 50 (RF50), 100 (RF100), 200 (RF200), 300 (RF300), 400 (RF400), and 500 (RF500), which are most commonly used in RF models<sup>14,29-31</sup>.

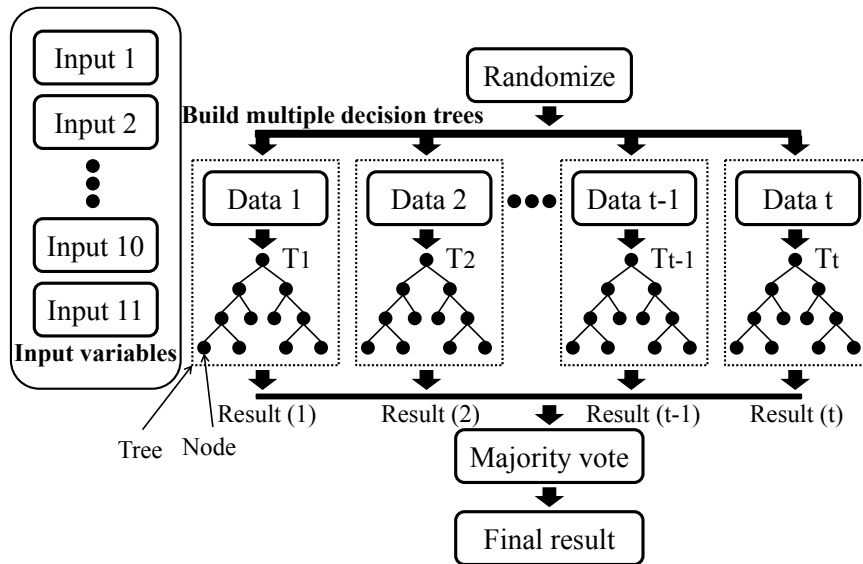


Figure 17. Algorithm of RF model

(D) Support vector machine (SVM)

Support vector machine is based on mapping data patterns in high dimensional

space through a kernel function. The data are divided into two groups by the training data called support vector<sup>17</sup>. An optimal SVM model is determined by choosing the maximum margin separation by the hyper-plane that separates support vector as shown in Figure 18<sup>32</sup>. Thus, the goal of the support vector machine is to improve the accuracy of a model by the optimization of separating space using a kernel function.

This study constructed mortality predicting models using kernel function of quadratic, polynomial, degree of 3 and 4, and Gaussian. Since there is no reliable methods for selecting suitable penalty parameter  $C$  and scaling factor  $\sigma$  of Gaussian kernel function, this study carried out exhaustive grid search changing penalty parameter  $C$  of 0.1, 1, and 10 and scaling factor  $\sigma$  of 0.1 and 1<sup>33,34</sup>.

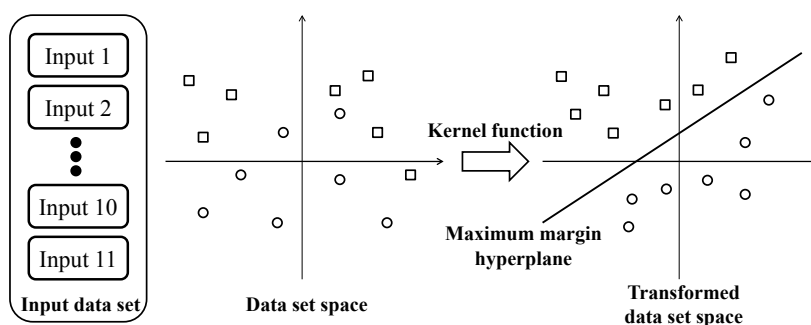


Figure 18. Algorithm of SVM model

#### (E) Advantages and disadvantages

Table 2 shows the advantages and disadvantages of the machine learning techniques used in this study.

Table 2. Advantages and disadvantages of LR, ANN, RF, and SVM

	Advantage	Disadvantage
LR	Statistical information (ex. odds ratio)	Not made for classification

ANN	Non linear regression	Local minima error
RF	Easy to use	Not allowed to examine individual trees separately
SVM	High performance	Required many settings

LR: logistic regression, ANN: artificial neural network, RF: random forest, SVM: support vector machine

## B. Model construction

### (A) Data set

For the models construction, this study obtained one data set from one rat. Therefore, 36 (1 data set \* 36 rats) data sets were obtained in this study (the numbers of the survival and death sets were 16 and 20, respectively). Thirty six data sets were divided randomly into mutually exclusive data sets. Among the data sets, 66.7% (n=24) were used as the training set to select optimal variables and construct the models, and the remaining 33.3% (n=12) were used in the model testing as listed in Table 3.

Table 3. Number of data sets for training and testing sets

	Training set	Testing set	Total set
Survival set	10	6	16
Death set	14	6	20
Total set	24	12	36

### (B) Variable selection

This study simultaneously performed variable selection with the grid search to optimize LR, ANN, RF, and SVM models as shown in Figure 19. This variable selection would be expected to reduce impression time of injured patients for first responders on scene. All the physiological variables, including HR, SBP,

DBP, MAP, PPR, TEMP, RR, LC, PP, SI, and NI were used as a candidate for variable selection. Basic concept of variable selection in this study was backward elimination using priority of the variables. Priority of the variables was determined based on embedded method of each machine learning techniques<sup>14,35</sup>. Then, 10-fold cross validation was repeated to calculate the mean accuracy of each cross validation process by progressively eliminating the least contributing ones until the most influential ones were left (backward elimination)<sup>36</sup>. The highest ranked variables with the best cross validated accuracy were chosen as the optimal variables. The predicting model was constructed using the optimal variables.

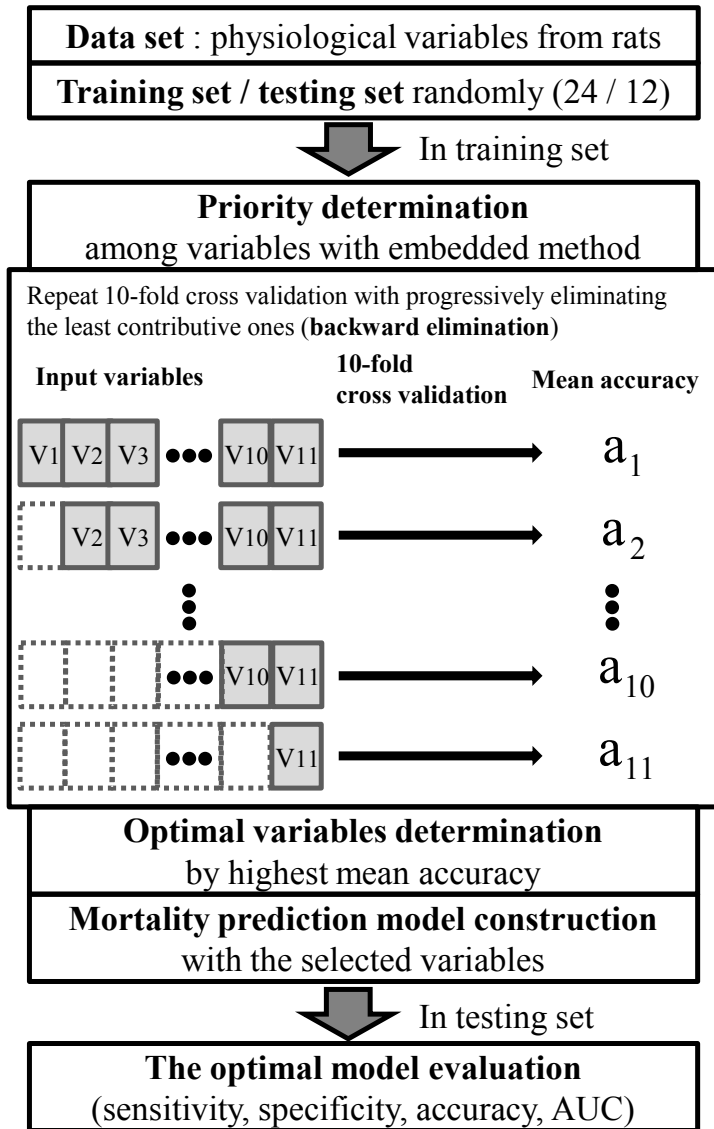


Figure 19. Flowchart of backward elimination variable selection and mortality predicting model construction

(C) Performance evaluation of the mortality predicting models

To compare the performance of mortality prediction models using the selected variables, this study obtained sensitivity, specificity, accuracy using the

remaining testing set. Definitions of these are as in the following (2), (3), and (4), respectively. This study also drew a ROC curve for each model and calculated the area under the ROC curve (AUC). ANN, RF, and SVM were analyzed using MATLAB software and LR was analyzed using SPSS 18.0.

$$\text{Sensitivity} = \frac{\text{TP}}{\text{TP} + \text{FN}} \quad (2)$$

$$\text{Specificity} = \frac{\text{TN}}{\text{FP} + \text{TN}} \quad (3)$$

$$\text{Accuracy} = \frac{\text{TP} + \text{TN}}{\text{TP} + \text{FP} + \text{TN} + \text{FN}} \quad (4)$$

Table 4. Used terminologies for sensitivity, specificity, accuracy in this study

	True death	True survival	Total
Predicting death	TP (true positive)	FP (false positive)	TP+FP
Predicting survival	FN (false negative)	TN (true negative)	FN+TN
Total	TP+FN	FP+TN	TP+FP+FN+TN

### III. RESULTS

#### 1. Experimental data resulting from hemorrhage

##### A. Experimental data for the survival and death groups

Table 5 shows the experimental data collected from 36 rats in the survival and death groups. A total of 16 rats survived, whereas 20 rats died. The mean (SD) percentages of bleeding for the survival and death groups were 42.3% (5.1%) and 51.2% (4.4%), respectively. In general, as controlled hemorrhage volume increased, tail bleeding decreased, except in the one surviving rat from the 3.0 mL/100 g group. None of the measured variables were significantly different between the survived and dead rat groups during the resting period, when assessed by the Mann-Whitney U test ( $P < 0.05$  for all variables).

Table 5. Experimental data for the survival and death groups<sup>13</sup>

	Survival group	Death group
n	16	20
Tail bleeding volume (mL/100 g), mean (SD)		
2.0 mL/100 g (n=12) (32.8%, amount of % controlled bleeding)	0.4 (0.1)	0.8 (0.5)
2.5 mL/100 g (n=12) (41.0%, amount of % controlled bleeding)	0.2 (0.2)	0.5 (0.3)
3.0 mL/100 g (n=12) (49.2%, amount of % controlled bleeding)	0.5*	0.3 (0.2)
% Tail bleeding, mean (SD)		
2.0 mL/100 g (32.8%, amount of % controlled bleeding)	7.0 (2.3)	13.3 (8.8)
2.5 mL/100 g (41.0%, amount of % controlled bleeding)	3.6 (2.9)	8.3 (4.2)
3.0 mL/100 g (49.2%, amount of % controlled bleeding)	7.8*	4.1 (2.4)
% Total bleeding, mean (SD)	42.3 (5.1)	51.2 (4.4)

% Tail bleeding = (tail bleeding volume / total blood volume) × 100%

\* One rat

## B. Changes in physiological data during hemorrhage

Figure 20 shows the changes in measured vital signs from 1 min before hemorrhage to 5 min after hemorrhage versus at rest. The vertical lines at 15 and 30 min indicate the start and cessation of the controlled hemorrhage, respectively. Heart rate slowly decreased during the initial hemorrhage, contrary to increases observed in hemorrhaging humans<sup>8,20</sup>. An HR increase during late hemorrhage in the death group was noticeable and was an expected compensatory mechanism for hypovolemia. Systolic BP and SI in both groups showed monotonous changes during hemorrhage. Therefore, these variables might be candidates for predicting mortality, because differences in these variables between the survival and death groups increased with time. Differences in SBP and SI (%) at 30 min between the survival and death groups were 24% and 244%, respectively in Table 6. Therefore, SI (%) was much more sensitive to hemorrhage than SBP alone.

Shock indices for both groups continuously increased until hemostasis was initiated at 30 min and maintained thereafter. The SI (%) of the death group increased much more rapidly than that of the survival group during hemorrhage, demonstrating more pronounced decreases in SBP for the death group. Among all tested variables, SBP and SI (%) showed the earliest significant differences between the survival and death groups. This difference became significant at 19 min, which was only 4 min after the controlled hemorrhage began.

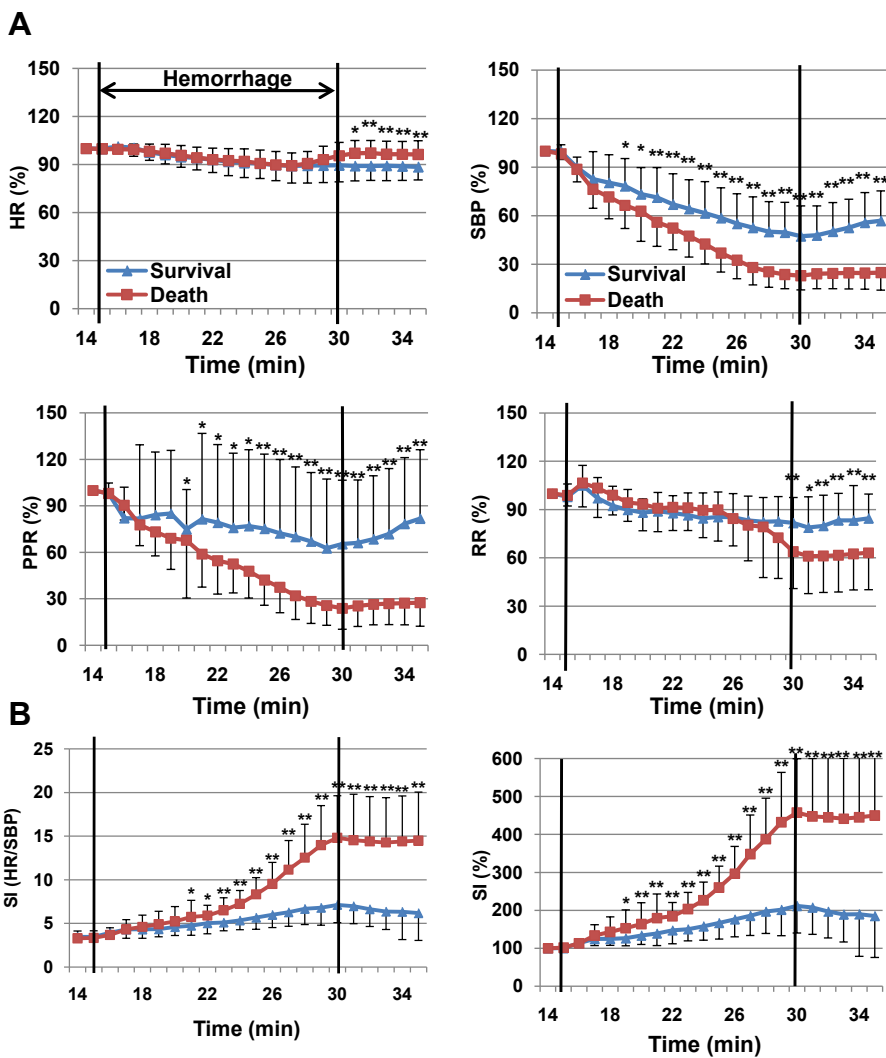


Figure 20. Relative changes in HR, SBP, PPR, and RR during hemorrhage (A), absolute values and relative changes in SI during hemorrhage (B)<sup>13</sup>, all values are percentages of the resting values, which were designated as 100%, error bars indicate standard deviation, HR: heart rate, SBP: systolic blood pressure, PPR: pulse pressure, RR: respiration rate, SI: shock index \*p<0.05, \*\*p<0.01

Figure 21 shows both the absolute and relative values (%) of LC, PP, and NI. The relative values, as percentages, for LC, PP, and NI showed greater significant differences between the survival and death groups than the absolute values. Accordingly, the following description was based on these relative values. Relative LCs were not significantly different between the survival and death groups until 26 min, which was 8 min later than SI (%). Although PP in both groups rapidly decreased until hemostasis began, PP in the survival group increased slowly after hemostasis, whereas PP in the death group roughly did not change.

There was a continuous significant difference in relative perfusion between the two groups beginning at 19 min, which was only 4 min after the hemorrhage began, which paralleled the early changes observed for SI (%). Importantly, as LC increased and PP decreased quickly during hemorrhage, the relative LC/PP ratio increased considerably, by more than 400% in the survival group and greater than 1,600% in the death group at the end of hemorrhage (Table 6). These considerable changes as a result of hemorrhage, as well as the early appearance of a significant difference between the two groups, suggest NI to be an attractive prognostic tool for surviving hemorrhagic shock.

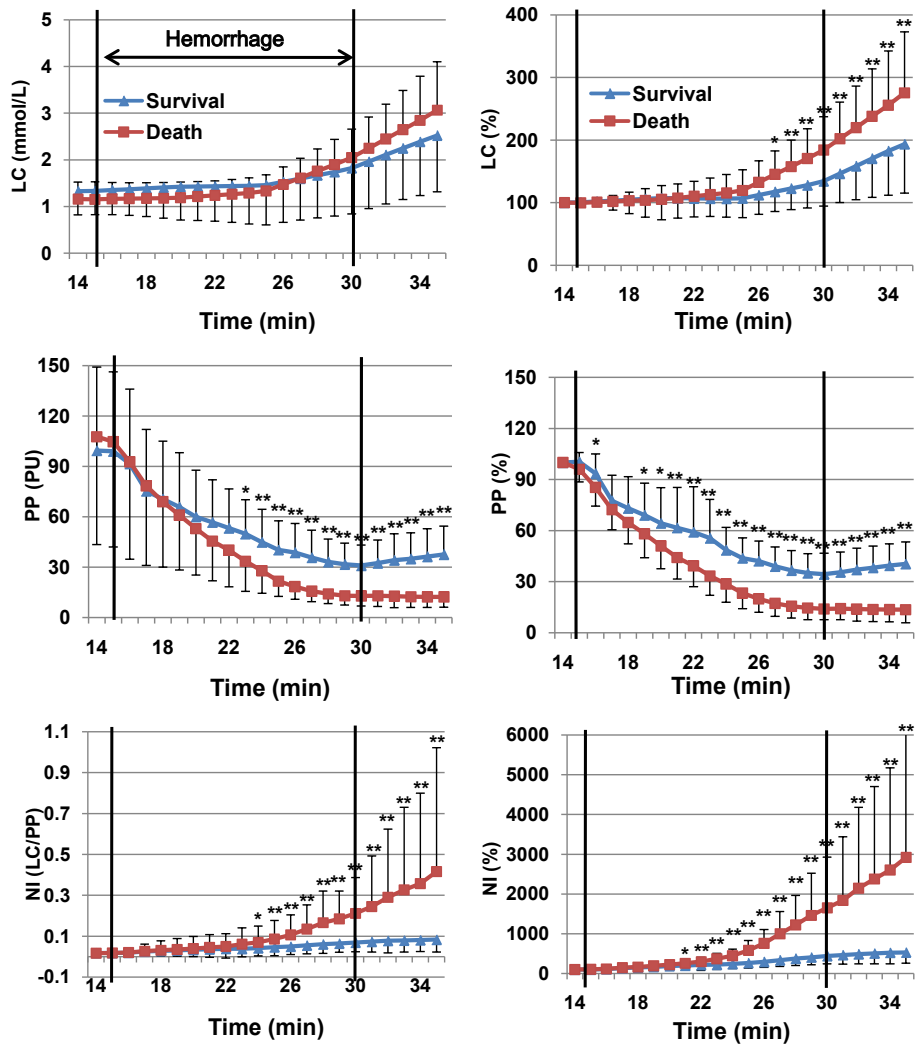


Figure 21. Absolute values (left column) and relative changes (right column) in LC, PP, and NI during hemorrhage<sup>13</sup>, all values in the right column are percentages of the resting values, which were designated as 100%, error bars indicate standard deviation, LC: lactate concentration, PP: peripheral perfusion, NI: new index \*p<0.05, \*\*p<0.01

### C. All measured data at the end of hemorrhage

Table 6 shows the percent changes in all measured data (mean (SD)) at the 30-min time point versus at rest (100 %) for both the survival and death groups. There were significant differences between the two groups for all variables ( $P < 0.05$ ), except for HR. The newly devised index demonstrated the following AUCs, in descending order of greatest value, of 0.975, 0.941, 0.922, 0.919, 0.903, 0.884, 0.847, 0.816, 0.783, 0.744, and 0.672 for NI, SI, PP, SBP, MAP, PPR, DBP, TEMP, LC, RR, and HR, respectively. Although PP and LC alone showed smaller AUCs than SI, NI showed the greatest AUC, as the ratio of LC to PP considerably increased with hemorrhage and minimized differences between individual animals. It is important to note that SI showed the second best AUC despite the small AUCs for HR and SBP alone, similar to that of NI.

Table 6. Comparison of all measured data (mean (SD),  $P$ ) at the end of hemorrhage between the survival and death groups and AUC data<sup>13</sup>

Variable, %	Survival (n=16)	Death (n=20)	$P$	AUC
NI (LC/PP)	437 (196)	1654 (1297)	<0.001*	0.975
SI (HR/SBP)	213 (72)	457 (143)	<0.001*	0.941
PP, PU	34 (12)	14 (9)	<0.001*	0.922
SBP, mmHg	47 (20)	23 (9)	<0.001*	0.919
MAP, mmHg	43 (16)	22 (9)	<0.001*	0.903
PPR, mmHg	65 (40)	24 (13)	<0.001*	0.884
DBP, mmHg	39 (16)	22 (9)	<0.001*	0.847
TEMP, °C	98 (1)	97 (1)	0.001*	0.816
LC, mmol/L	132 (40)	181 (54)	0.004*	0.783
RR, breaths/min	81 (16)	64 (22)	0.013*	0.744
HR, beats/min	90 (12)	95 (9)	0.080	0.672

\* $P < 0.05$ , PU: perfusion unit

#### D. Correlation coefficients of all measured data with mortality

Table 7 shows the correlation coefficients of all of the variables with mortality using Spearman rank test. All variables except for HR exhibited statistically significant correlation coefficients ( $P < 0.05$ ). The rank order of the correlation coefficients was exactly the same as that for the AUCs of these variables.

Table 7. Correlation coefficients of all variables with mortality<sup>13</sup>

Variable	Correlation coefficient	<i>P</i>
NI	-0.818	<0.001*
SI	-0.759	<0.001*
PP	0.726	<0.001*
SBP	0.721	<0.001*
MAP	0.694	<0.001*
PPR	0.662	<0.001*
DBP	0.597	<0.001*
TEMP	0.544	0.001*
LC	-0.487	0.003*
RR	0.420	0.011*
HR	-0.296	0.080

## 2. Variable selection and performance of the mortality predicting models

### A. Logistic regression

#### (A) Selected variables in the training set and ROC curve of LR model

TEMP, LC, and SI were selected in LR backward variable selection for constructing the optimal LR model.

For the LR model, sensitivity, specificity, accuracy, and AUC were 0.678, 1.000, 0.833, and 0.833, respectively. Figure 22 shows the ROC curve for the optimal LR model.

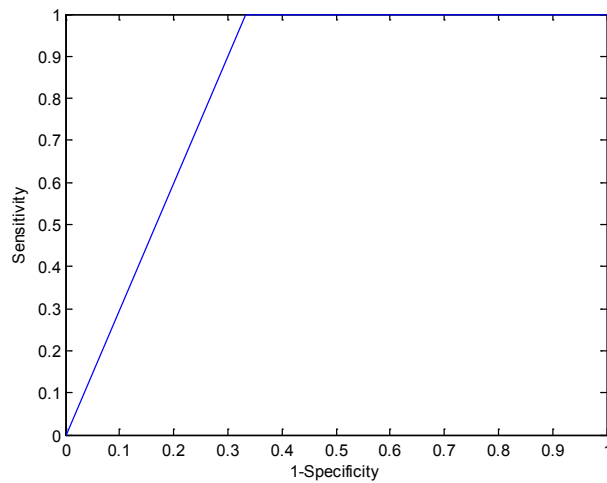


Figure 22. Receiver operating characteristic curve of LR model

## B. Artificial neural network

### (A) Selected variables in the training set

Table 8 shows the selected variables and accuracy in ANN models with the different number of hidden neurons using 10-fold cross validation in the training set. All the cases of hidden neurons except the number of 7 showed the same accuracy in variable selection. This study demonstrated all the number of hidden neurons except that of 7 in the testing set to determine the optimal performance of an ANN model.

Table 8. Selected variables and accuracy for ANN models in the training set

	HR	SBP	DBP	MAP	PPR	RR	TEMP	LC	PP	SI	NI	ACC
N2										○		1.00
N3	○							○		○		1.00
N4										○		1.00
N5										○		1.00
N6										○		1.00
N7	○							○		○		0.95
N8	○	○		○				○		○	○	1.00
N9	○	○						○		○		1.00
N10										○		1.00

*N<sub>n</sub>*: number of hidden neurons, ACC: accuracy

### (B) Performance of the mortality predicting model in the testing set

Table 9 shows the performance of the ANN models with the selected different number of hidden neurons using the testing set. The ANN model with 3 hidden neurons showed the best performance among the others. Sensitivity, specificity, accuracy, and AUC for the optimal ANN model were 0.833, 1.000, 0.917, and

0.917, respectively.

Figure 23 shows the receiver operating characteristic curve for the optimal ANN model with 3 hidden neurons.

Table 9. Performance of the ANN models with the different number of hidden neurons in the testing set

	Sensitivity	Specificity	Accuracy	AUC
N2	0.833	1.000	0.917	0.861
N3	0.833	1.000	0.917	0.917
N4	0.833	1.000	0.917	0.861
N5	0.833	1.000	0.917	0.861
N6	0.833	1.000	0.917	0.861
N8	0.833	0.833	0.833	0.833
N9	0.833	1.000	0.917	0.861
N10	0.833	0.833	0.833	0.833

$Nn$ : number of hidden neurons

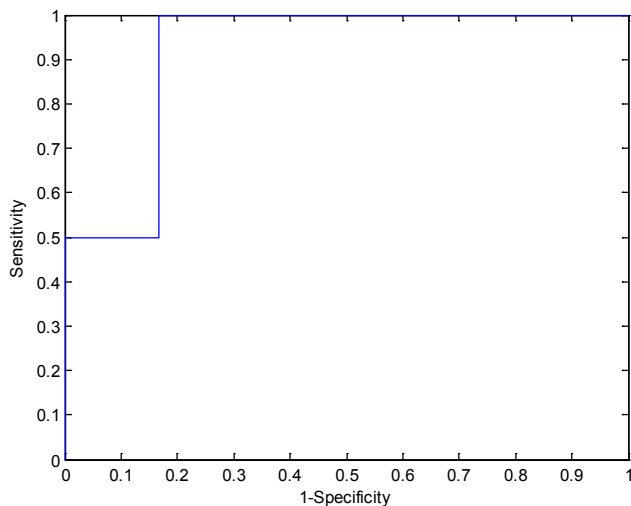


Figure 23. Receiver operating characteristic curve of ANN model with 3 hidden neurons

### C. Random forest

#### (A) Selected variables in the training set

Table 10 shows the selected variables and accuracy in RF models with the different number of trees using 10-fold cross validation in the training set. All RF models designed in this study selected SI and showed the same accuracy in variable selection. This study demonstrated all the designed number of trees in the testing set to determine the optimal performance of a RF model.

Table 10. Selected variables and accuracy for RF models with different number of trees in the training set

	HR	SBP	DBP	MAP	PPR	RR	TEMP	LC	PP	SI	NI	ACC
RF50										○		0.95
RF100										○		0.95
RF200										○		0.95
RF300										○		0.95
RF400										○		0.95
RF500										○		0.95

RF*n*: number of trees, ACC: accuracy

#### (B) Performance of the mortality predicting model in the testing set

Table 11 shows the performance of the RF models with 50, 100, 200, 300, 400, and 500 trees in the testing set. The RF model with 100 trees showed the best performance among the others. Sensitivity, specificity, accuracy, and AUC for the optimal RF model were 0.833, 1.000, 0.917, and 0.903, respectively.

Figure 24 shows the receiver operating characteristic curve for the optimal RF model with 100 trees.

Table 11. Performance of the RF models with different number of trees in the testing set

	Sensitivity	Specificity	Accuracy	AUC
RF50	0.833	1.000	0.917	0.875
RF100	0.833	1.000	0.917	0.903
RF200	0.833	1.000	0.917	0.875
RF300	0.833	1.000	0.917	0.875
RF400	0.833	1.000	0.917	0.875
RF500	0.833	1.000	0.917	0.875

RF*n*: number of trees

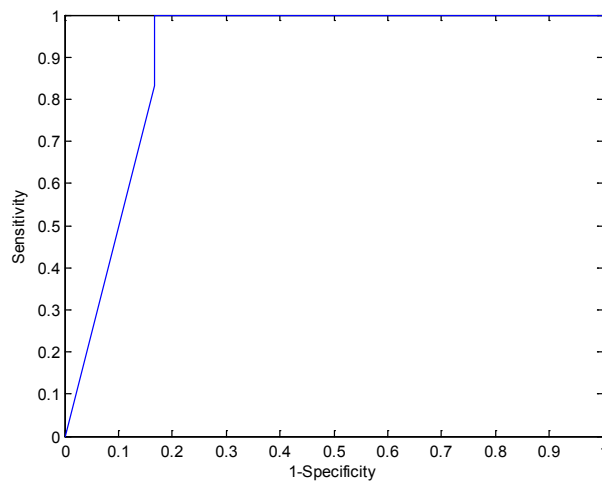


Figure 24. Receiver operating characteristic curve of RF model with 100 trees

## D. Support vector machine

### (A) Selected variables in the training set

Table 12 shows the selected variables and accuracy in SVM models with the different kernel function using 10-fold cross validation in the training set. SVM models with the kernel function, except different three parameters of Gaussian kernel function, showed the same high accuracy in variable selection. This study demonstrated SVM models using the selected kernel function and variables to determine the optimal performance of a SVM model in the testing set.

Table 12. Selected variables and accuracy for SVM models with the different kernel function in the training set

	HR	SBP	DBP	MAP	PPR	RR	TEMP	LC	PP	SI	NI	ACC
Quadra								○			○	1.00
Poly 3							○	○	○		○	1.00
Poly 4	○	○		○			○	○	○	○	○	1.00
RBF (0.1/0.1)											○	0.90
RBF (0.1/1)								○			○	1.00
RBF (1/0.1)											○	0.90
RBF (1/1)							○	○	○	○	○	1.00
RBF (10/0.1)											○	0.85
RBF (10/1)							○	○	○	○	○	1.00

Quadra: quadratic, Poly: polynomial,

RBF ( $n/m$ ): Gaussian (penalty parameter/scaling factor), ACC: accuracy

### (B) Performance of the mortality predicting model in the testing set

Table 13 shows the performance of the SVM models with the selected

different kernel function and variables using the testing set. The SVM model using Gaussian kernel function with penalty parameter of 0.1 and scaling factor of 1 showed the best performance among the others. Sensitivity, specificity, accuracy, and AUC for the optimal SVM model were 1.000, 0.833, 0.917, and 0.972, respectively.

Figure 25 shows the receiver operating characteristic curve for the optimal SVM model using Gaussian kernel function with penalty parameter of 0.1 and scaling factor of 1.

Table 13. Performance of the SVM models with the different kernel function in the testing set

	Sensitivity	Specificity	Accuracy	AUC
Quadra	0.833	1.000	0.917	0.833
Poly 3	0.500	1.000	0.750	0.611
Poly 4	0.833	1.000	0.917	0.833
RBF (0.1/1)	1.000	0.833	0.917	0.972
RBF (1/1)	0.833	1.000	0.917	0.944
RBF (10/1)	0.833	1.000	0.917	0.833

Quadra: quadratic, Poly: polynomial,

RBF ( $n/m$ ): Gaussian (penalty parameter/scaling factor)

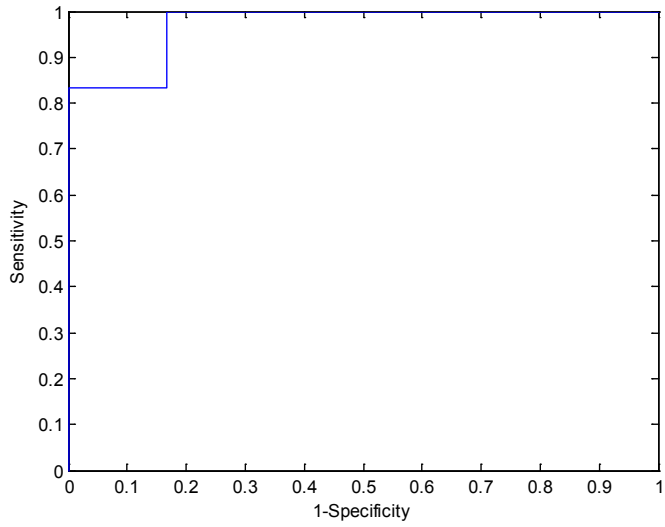


Figure 25. Receiver operating characteristic curve of SVM model using Gaussian kernel function with penalty parameter of 0.1 and scaling factor of 1

### 3. Optimal mortality predicting model selection for hemorrhagic shock

Optimal ANN, RF, and SVM models showed greater accuracy and AUC than those of LR model. Since LR models are currently used as gold standard to demonstrate diagnostic predicting models suggested in many machine learning studies, all the ANN, SVM, and RF models might be suitable for mortality predicting models resulting from hemorrhagic shock in this study. It is important to note that only the SVM model showed greater sensitivity than specificity among the models. In this study designed for mortality predicting models, sensitivity meant the probability of death in rats correctly identified as dead due to hemorrhage. The SVM model was more useful for predicting mortality in a rat model than others. Although ANN, RF, and SVM models showed the same accuracy for predicting mortality, the SVM model showed the greatest AUC compared to other models. Generally AUC is a better measure than accuracy in evaluating learning algorithms<sup>37</sup>. Therefore, the SVM model was superior to LR, ANN, and RF models in terms of sensitivity and AUC in this study.

#### IV. DISCUSSION

Variable selection methods have been conducted in many studies to optimize diagnostic models and to determine informative risk factors for certain diseases among various factors in the clinical setting<sup>14,35</sup>. This study applied variable selection to diagnose acute hemorrhagic shock not only to make the optimal mortality predicting models but also to find more influential physiologic variables for acute hemorrhagic shock. As the results, variables including LC, SI, and NI were selected in the LR, ANN, RF, and SVM models.

The ATLS for Doctors (Student Manual) suggests that shock severity can be classified by conventional vital signs<sup>20</sup>. However, many studies have indicated that the ATLS classification is unsatisfactory for classifying shock severity. Guly et al.<sup>8</sup> tested the validity of ATLS classification using a database of injury and outcome variables in injured adult patients. They reported that there was a trend toward increasing HR and decreasing SBP with increasing estimated blood loss, but not to the degree suggested by the ATLS. In fact, SI, defined as the ratio of HR to SBP, may be more useful to diagnose early hemorrhagic shock than either HR or SBP alone, and may facilitate the earlier identification of a relatively high-risk hemorrhage in injured patients in the pre-hospital setting<sup>7</sup>.

In our study, SI demonstrated better performance in predicting mortality resulting from hemorrhage than conventional vital signs and was significantly different between survival and death groups at an earlier time point than even NI. In addition, SI has an advantage in terms of its rapid response to hemostasis as shown in Figure 20. After hemostasis, SIs in both groups stopped their increases and began to slowly decrease. Shock index value would be a good indicator for evaluating hemostasis in emergency rooms, in agreement with previous results<sup>7</sup>.

However, measurement of SBP, a component of SI, entails some difficulties for first responders in the field. Blood pressure measurement via a cuff can be impeded by extremity injuries, is often inaccurate in children, and can differ

according to age and posture. Cuff size is also a leading cause of error in BP measurement<sup>38,39</sup>. Conducting BP measurement in a pre-hospital setting requires a high degree of clinical experience and involves a high degree of error that increases with an SBP lower than 90 mmHg<sup>39</sup>. Therefore, although SI showed the second best AUC, its usage could be limited in the field or pre-hospital settings.

The new severity index, defined as the LC/PP ratio, showed the best performance in regard to AUC, correlation coefficient for predicting mortality, and variable selection in the SVM model. As a product of anaerobic glycolysis, LC indicates indirectly oxygen debt. Many studies have selected LC to determine the presence of tissue ischemia for predicting severity in hemorrhagic shock<sup>6,9</sup>. Not et al.<sup>24</sup> investigated changes in serum LC as marker of metabolic acidosis in a lethal hemorrhagic rat model (55% hemorrhage of total blood volume) to evaluate the effect of glucosamine on survival time. They reported that there were significant increases in serum LC in response to hemorrhage. Reynolds et al.<sup>40</sup> also reported that increased LC is a key feature of lethal hemorrhagic shock. Although LC slowly increased with hemorrhage in our study, it demonstrated a possibility for use in predicting the severity of hemorrhagic shock. In recent years, new portable lactate analyzers have been developed, offering measurements in no more than a few minutes, and have exhibited high correlation with traditional serum LC measurement<sup>6</sup>. The device we used to measure blood LC does not require professional skill, and results can be obtained within 60 s. This study measured LC to predict lethal shock severity using a portable lactate analyzer to calculate NI.

Many studies have monitored microcirculation to diagnose hemorrhagic shock using laser Doppler flowmetry as a marker of tissue hypoperfusion<sup>21</sup>. In this study, PP showed early decreases and significant differences between the survival and death groups during hemorrhage. Kaiser et al.<sup>38</sup> reported that PP responded to severe hemorrhage earlier than BP in a swine model. The advantages of laser Doppler flowmetry include less complexity, noninvasiveness, and the ability to continuously monitor microcirculatory blood

flow in real time<sup>21</sup>. The skin is the first organ to be limited in blood supply during hemorrhage to maintain blood supply to crucial organs such as the brain or lungs. In addition, several studies reported that measuring superficial dermal capillary blood flow could detect early hemorrhage<sup>38</sup>. Accordingly, this study monitored peripheral superficial dermal capillary microcirculation in the skin of the right front sole as a measure of PP to calculate NI.

As seen in Table 6, NI showed a 1217% difference between the survival and death groups, even though PP and LC showed very small differences of 20% and 49%, respectively. This large difference in NI resulted from a decrease in the denominator (PP) and an increase in the numerator (LC) when calculating NI. This is the main reason why NI is more attractive for predicting mortality during acute hemorrhage. Another merit of NI is the minimization of differences between individual animals.

The major clinical importance of NI is as follows: First, NI is easy to use in the field. NI measurement does not require professional skill. Second, NI can indicate potentially lethal damage to the body due to hemorrhage. NI reflects tissue ischemia via LC and tissue hypo-perfusion via PP, whereas SI reflects cardiac compensation. As shown in Figure 20B, SIs in both groups stopped their increase after hemostasis. Whereas NI in the survival group very slowly increased after hemostasis, the NI of the death group rapidly increased despite hemostasis, as seen in Figure 21.

Pickering et al.<sup>39</sup> reported that establishment of trends in BP before arriving at the hospital is more important than the absolute values of BP in the pre-hospital setting, which is often inaccurately measured. If one were to consider only the trends in SI (%) seen in Figure 20B, it would be hard to predict whether the rats belonged to the death group (lethal condition) or the survival group (severe condition), especially after hemostasis. However, as shown in Figure 21, NI (%) rapidly increased between a few intervals regardless of hemostasis, indicating that the rats would involve a more fatal condition in terms of tissue damage; slight increases in NI would indicate a good chance of survival. Therefore, NI would be a better indicator for predicting the lethal severity of a hemorrhage

than SI.

In this study, neither a larger number of trees showed different variable selection nor demonstrated improved performance in general. Archer<sup>29</sup> and Albert<sup>30</sup> et al. reported that the number of trees must be chosen large enough to get stable estimates of variable importance. On the other hand, Chen<sup>31</sup> and Ham<sup>41</sup> et al. reported that a larger number of trees did not provide improved performance. Validation for the number of trees is warranted in future study. Support vector machine, especially using Gaussian kernel function, is well known for its high performance to diagnose diseases as a machine learning technique<sup>42</sup>. In this study, the SVM model using Gaussian kernel function demonstrated the best performance on predicting mortality due to hemorrhagic shock in a rat model. It is expected to use SVM to diagnose hemorrhagic shock severity in human for the future study.

This study showed that ATLS class IV hemorrhagic shock could be further classified into two subclasses. In Table 5, the mean hemorrhagic volumes for the survival and death groups were 42.3% (5.1%) and 51.2% (4.4%), respectively, and these were classified as class IV according to the ATLS shock classification currently used in the clinical setting. Macias et al.<sup>23</sup> divided rats into severe and lethal hemorrhage groups according to hemorrhage volumes of 40% and 51.6%, respectively, and showed different survival times between the two groups. The hemorrhage volumes used in Macias' study were very similar to those of our survival and death groups. Comparing our results with Macias' study, ATLS class IV could be subdivided into two classes. If class IV is subdivided into a severe hemorrhage group, which would be equivalent to our survival group, and a lethal hemorrhage group, equivalent to our death group, it might be clinically helpful to predict severity and make decisions for treatment in class IV hemorrhagic shock.

Another noticeable finding of this study was that the relative values for SI, LC, PP, and NI indicated significant differences between the survival and death groups earlier than the absolute values thereof during hemorrhage. This finding may be very helpful for first responders in the field, but future study to confirm

this finding in humans is warranted.

There were several limitations to our study. First, we used a 15-min bleeding time to simulate ambulance response times before initial on-scene patient contact. However, it is possible that initial contact would take less or more than 15 min. Therefore, it is warranted to investigate mortality applying NI for different hemorrhage times. Second, the laser Doppler system used to measure perfusion is expensive and sensitive to motion artifacts. Development of a technique to reduce motion artifacts with some type of fixture that can maintain stable contact with skin would be helpful to future study. Third, this study did not perform any resuscitation. We originally conducted this study to more accurately reflect the clinical impression encountered by first responders in the battlefield or instances of civilian trauma. NI could be useful to first responders for clinically predicting the severity of hemorrhage and determining the priority of treatment and proper resuscitation simultaneously with SI or conventional vital signs. Therefore, it is warranted to investigate the effects of resuscitation on NI in a future study.

Fourth, validation study for humans is needed. For example, HR did not increase in our rat model during initial hemorrhage, which showed a similar result with Letson's<sup>3</sup> earlier rat study. Swine models of acute hemorrhage showed similar trends of no increases in HR with blood loss until 50%<sup>10,43</sup>, contrary to human studies<sup>8,20</sup>. Pestel et al.<sup>10</sup> reported that such lack of tachycardia with blood loss might be caused by isoflurane anesthesia. In humans, SI would be different from that of rats because HR is directly related to SI. However, NI may be less different in humans from that of rats than SI because NI is not directly related to HR.

Fifth, although this study used only 36 data sets, statistical power of SI and NI were 1 and 0.977, respectively. Many studies control statistical power up to 0.8 in order to verify the minimum sample size required<sup>44</sup>. Finally, we analyzed these variables based on their changes between rest and following hemorrhage to predict mortality in rats. In emergency situations, one would not be provided with resting variable measurements, and we should replace resting variables

with normally distributed data ranges for humans.

## V. CONCLUSION

In conclusion, support vector machine of this study showed better performance in regard to sensitivity and AUC in comparison to other machine learning techniques in acute lethal hemorrhagic shock in rats. Even though the support vector machine is not applicable to humans at present, this study showed its potential as a promising technique for clinical application. If confirmation of this support vector machine as a better diagnostic tool in clinical situations is provided, this technique could be helpful to first responders for clinically predicting lethal hemorrhagic shock in instances of civilian trauma or on the battlefield.

## REFERENCES

1. World Health Organization: World health statistics 2012, World Health Organization Press: 62-70, 2012.
2. Kauvar DS, Lefering R, Wade CE. Impact of hemorrhage on trauma outcome: an overview of epidemiology, clinical presentations, and therapeutic considerations. *J Trauma* 2006; 60 (Suppl):3-11.
3. Letson HL, Dobson GP. Unexpected 100% survival following 60% blood loss using small-volume 7.5% NaCl with adenocaine and Mg(2+) in the rat model of extreme hemorrhagic shock. *Shock* 2011; 36:586-94.
4. Lerner EB, Schwartz RB, Coule PL, Weinstein ES, Cone DC, Hunt RC, et al. Mass casualty triage: an evaluation of the data and development of a proposed national guideline. *Disaster Med Public Health Prep* 2008; 2 (Suppl):25-34.
5. Benedek DM, Fullerton C, Ursano RJ. First responders: mental health consequences of natural and human-made disasters for public health and public safety workers. *Annu Rev Public Health* 2007; 28:55-68.
6. Wilson M, Davis DP, Coimbra R. Diagnosis and monitoring of hemorrhagic shock during the initial resuscitation of multiple trauma patients: a review. *J Emerg Med* 2003; 24:413-22.
7. Vandromme MJ, Griffin RL, Weinberg JA, Rue LW 3rd, Kerby JD. Lactate is a better predictor than systolic blood pressure for determining blood requirement and mortality: could prehospital measures improve trauma triage? *J Am Coll Surg* 2010; 210:861-7, 867-9.
8. Guly HR, Bouamra O, Spiers M, Dark P, Coats T, Lecky FE. Vital signs and estimated blood loss in patients with major trauma: testing the validity of the ATLS classification of hypovolaemic shock. *Resuscitation* 2011; 82:556-9.
9. Dutton RP. Current concepts in hemorrhagic shock. *Anesthesiol Clin* 2007; 25:23-34.
10. Pestel GJ, Fukui K, Kimberger O, Hager H, Kurz A, Hildebrand LB. Hemodynamic parameters change earlier than tissue oxygen tension in hemorrhage. *J Surg Res* 2010; 160:288-93.
11. Birkhahn RH, Gaeta TJ, Terry D, Bove JJ, Tloczkowski J. Shock index in diagnosing early acute hypovolemia. *Am J Emerg Med* 2005; 23:323-6.
12. Nakasone Y, Ikeda O, Yamashita Y, Kudoh K, Shigematsu Y, Harada K. Shock index correlates with extravasation on angiographs of gastrointestinal hemorrhage: a logistics regression analysis. *Cardiovasc Inter Rad* 2007; 30:861-5.
13. Choi JY, Lee WH, Yoo TK, Park I, Kim DW. A new severity predicting index for hemorrhagic shock using lactate concentration and peripheral perfusion in a rat model. *Shock* 2012; 38:635-41.
14. Hsieh CH, Lu RF, Lee NH, Chiu WT, Hsu MH, Li YC. Novel solutions for an old

- disease: diagnosis of acute appendicitis with random forest, support vector machines, and artificial neural networks. *Surgery* 2011; 149:87–93.
15. Roberts DA, Holcomb JB, Parker BE, Jr., Sodeen JL, Pusateri AE, Brady WJ, Jr., et al. The use of polynomial neural networks for mortality prediction in uncontrolled venous and arterial hemorrhage. *J Trauma* 2002; 52:130-5.
  16. Eftekhari B, Mohammad K, Ardebili HE, Ghodsi M, Ketabchi E. Comparison of artificial neural network and logistic regression models for prediction of mortality in head trauma based on initial clinical data. *BMC Med Inform and Decis Mak* 2005; 5:3.
  17. Jang KH, Yoo TK, Choi JY, Nam KC, Choi JL, Kwon MK, et al. Comparison of survival predictions for rats with hemorrhagic shocks using an artificial neural network and support vector machine. *Conf Proc IEEE Eng Med Biol Soc. Boston* 2011; 2011:91-4.
  18. Choi JY, Kim SK, Lee WH, Yoo TK, Kim DW. A survival prediction model of rats in hemorrhagic shock using the random forest classifier. *Conf Proc IEEE Eng Med Biol Soc. San Diego* 2012; 2012:5570-3.
  19. Yang S, Zou LY, Bounelis P, Chaudry I, Chatham JC, Marchase RB. Glucosamine administration during resuscitation improves organ function after trauma hemorrhage. *Shock* 2006; 25:600-7.
  20. American College of Surgeons Trauma Committee. *Advanced trauma life support for doctors*. 8th ed. Chicago (IL): Am Coll of Surg; 2008.
  21. Lima A, Bakker J. Noninvasive monitoring of peripheral perfusion. *Intensive Care Med* 2005; 31:1316-26.
  22. Leahy MJ, de Mul FF, Nilsson GE, Maniewski R. Principles and practice of the laser-Doppler perfusion technique. *Technol Health Care* 1999; 7:143-62.
  23. Macias CA, Kameneva MV, Tenhunen JJ, Puyana JC, Fink MP. Survival in a rat model of lethal hemorrhagic shock is prolonged following resuscitation with a small volume of a solution containing a drag-reducing polymer derived from aloe vera. *Shock* 2004; 22:151-6.
  24. Not LG, Marchase RB, Fulop N, Brocks CA, Chatham JC. Glucosamine administration improves survival rate after severe hemorrhagic shock combined with trauma in rats. *Shock* 2007; 28:345-52.
  25. Takasu A, Sakamoto T, Okada Y. Effect of induction rate for mild hypothermia on survival time during uncontrolled hemorrhagic shock in rats. *J Trauma* 2006; 61:1330-5.
  26. Ahn JO: *Statistical analysis of biomedical data using SPSS 18.0 [in EMR & PHP system]*. Seoul, Korea: Hannarae Publishing Co; 2010.
  27. Goyal NK, Kumar A, Trivedi S, Dwivedi US, Singh TN, Singh PB. A comparative study of artificial neural network and multivariate regression analysis to analyze

- optimum renal stone fragmentation by extracorporeal shock wave lithotripsy. *Saudi J Kidney Dis Transpl* 2010; 21:1073-80.
28. Basheer IA, Hajmeer M. Artificial neural networks: fundamentals, computing, design, and application. *J Microbiol Methods* 2000; 43:3-31.
  29. Archer KJ, Kimes RV. Empirical characterization of random forest variable importance measures. *Comput Stat Data An* 2008; 52:2249-60.
  30. Albert J, Aliu E, Anderhub H, Antoranz P, Armada A, Asensio M, et al. Implementation of the random forest method for the imaging atmospheric Cherenkov telescope MAGIC. *Nucl Instrum Meth A* 2008; 588: 424-32.
  31. Chen XW, Liu M. Prediction of protein-protein interactions using random decision forest framework. *Bioinformatics* 2005; 21:4394-400.
  32. Cortes C, Vapnik V. Support-vector networks. *Mach Learn* 1995; 20:273-97.
  33. Friedrichs F, Igel C. Evolutionary tuning of multiple SVM parameters. *Neurocomputing* 2005; 64:107-17.
  34. Manikandan J, Venkataramani B. Study and evaluation of a multi-class SVM classifier using diminishing learning technique. *Neurocomputing* 2010; 73:1676-85.
  35. Saeys Y, Inza I, Larrañaga P. A review of feature selection techniques in bioinformatics. *Bioinformatics* 2007; 23:2507-17.
  36. Dash M, Liu H. Consistency-based search in feature selection. *Artif Intell* 2003; 151:155-76.
  37. Huang J, Ling CX. Using AUC and accuracy in evaluating learning algorithms. *IEEE Trans Knowl Data Eng* 2005; 17:299-310.
  38. Kaiser ML, Kong AP, Steward E, Whealon M, Patel M, Hoyt DB, et al. Laser Doppler imaging for early detection of hemorrhage. *J Trauma* 2011; 71:401-6.
  39. Pickering TG, Hall JE, Appel LJ, Falkner BE, Graves J, Hill MN, et al. Recommendations for blood pressure measurement in humans and experimental animals: part 1: blood pressure measurement in humans: a statement for professionals from the subcommittee of professional and public education of the American heart association council on high blood pressure research. *Circulation* 2005; 8:697-716.
  40. Reynolds PS, Barbee RW, Skaflen MD, Ward KR. Low-volume resuscitation cocktail extends survival after severe hemorrhagic shock. *Shock* 2007; 28:45-52.
  41. Ham J, Chen Y, Crawford MM, Ghosh J. Investigation of the random forest framework for classification of hyperspectral data. *IEEE Trans Geosci Remote* 2005; 43:492-501.
  42. Zhao ZD, Lou YY, Ni JH, Zhang J. RBF SVM and its application on reliability evaluation of electric power system communication network. *Conf Proc Mach Learn Cybern. Baoding* 2012; 2012:91-4.
  43. Frankel DA, Acosta JA, Anjaria DJ, Porcides RD, Wolf PL, Coimbra R, et al.

Physiologic response to hemorrhagic shock depends on rate and means of hemorrhage. *J Surg Res* 2007; 142:276-80.

44. Moher D, Dulberg CS, Wells GA. Statistical power, sample size, and their reporting in randomized controlled trials. *JAMA* 1992; 272:122-4.

<ABSTRACT (IN KOREAN)>

다양한 기계 학습법을 이용한 급성 출혈성 쇼크의 환귀에서의  
사망 예측 모델

<지도교수 김 덕 원>

연세대학교 대학원 의과학과

최 준 열

전쟁 시 또는 사고 현장에서 환자의 중증도를 정확히 판단하는 것은 환자의 생명을 살리는데 매우 중요하다. 그러나, 사망예측에 중요한 생리학적 변수의 선정과 다양한 기계 학습법 중 가장 적합한 기계 학습법을 비교한 연구는 없는 실정이다. 본 연구는 다양한 기계 학습법을 이용하여 급성 출혈성 쇼크의 환귀에서의 사망 예측 모델을 제시함으로써 응급의료진이 현장에서 환자의 중증도를 정확히 판단하는데 도움이 되고자 하였다. 또한 출혈성 쇼크로 인한 사망 예측에 중요한 생리학적 변수를 선정하여 가능한 진단 시간을 줄이고자 하였다.

환귀 36 마리를 제어 출혈량에 따라 무작위로 12 마리씩 나누는 후, 제어 출혈과 함께 꼬리를 절단하여 비제어 출혈을 유도하였다. 본 연구에서는 심박수, 수축기 혈압, 이완기 혈압, 평균 동맥압, 맥압, 호흡수, 체온, 젖산 농도, 말초관류, 쇼크 인덱스 및 본 연구에서 제안한 새로운 중증도 예측 인덱스를 측정하여 변수 선정의 후보로 사용하였다. 모든 데이터는 출혈에 의한 영향을 관찰하기 위하여 출혈 직전과 출혈 직후의 변화를 비교 하였다. 훈련 데이터는 가장 널리 쓰이는 기계 학습법인 회귀분석, 인공신경망, 랜덤 포리스트, 지원 벡터 기계 모델을 형성하는데 사용하였다. 또한 각 모델의 입력 변수 선정을 위하여 10-fold cross validation을 이용한 변수 제거법을 사용하여 변수들을 선정하였다. 테스트 데이터는 선정된 변수로 구성된 최적화 된 모델들의 성능을 평가하기 위해 사용하였으며 이를 위해 민감도, 특이도, 정확도 및 AUC를 비교하였다.

최적화 된 회귀분석 모델의 민감도, 특이도, 정확도 및 AUC는 각각 0.678, 1.000, 0.833과 0.833이었다. 인공신경망 모델의 민감도, 특이도, 정확도 및 AUC는 각각 0.833, 1.000, 0.917과 0.917이었다. 또한 랜덤 포리스트 모델의 민감도, 특이도, 정확도 및 AUC는 각각 0.833, 1.000, 0.917과 0.903이었다. 마지막으로 지원 벡터 기계 모델의 민감도, 특이도, 정확도 및 AUC는 각각

1.000, 0.833, 0.917 및 0.972로서 지원 벡터 기계 모델이 회귀분석, 인공신경망, 랜덤포리스트 모델보다 높은 AUC를 보였다. 이 때 지원 벡터 기계 모델에 선정된 변수는 젓산 농도와 새로운 중증도 예측 인덱스이었다.

결론적으로 젓산 농도, 새로운 중증도 예측 인덱스로 구성된 지원 벡터 기계 모델이 출혈성 쇼크로 인한 사망예측에 회귀분석, 인공신경망, 랜덤포리스트 모델보다 우수한 성능을 보였다. 이러한 기계 학습법은 추후 전쟁 시 또는 사고 현장에서 응급 의료진에게 출혈성 쇼크의 환자의 정확한 중증도 예측 및 적절한 치료를 하는데 도움이 될 것으로 사료된다.

---

핵심되는 말 : 출혈성 쇼크, 혼귀, 새로운 인덱스, 쇼크 인덱스, 기계 학습법, 지원 벡터 기계, 랜덤 포리스트

## PUBLICATION LIST

### **International journal**

**Choi JY**, Lee WH, Yoo TK, Park I, Kim DW. A new severity predicting index for hemorrhagic shock using lactate concentration and peripheral perfusion in a rat model. Shock 2012; 38:635-41.

### **International conference proceedings**

**Choi JY**, Kim SK, Lee WH, Yoo TK, Kim DW. A survival prediction model of rats in hemorrhagic shock using the random forest classifier. Conf Proc IEEE Eng Med Biol Soc. San Diego 2012; 2012:5570-3.

Jang KH, Yoo TK, **Choi JY**, Nam KC, Choi JL, Kwon MK, et al. Comparison of survival predictions for rats with hemorrhagic shocks using an artificial neural network and support vector machine. Conf Proc IEEE Eng Med Biol Soc. Boston 2011; 2011:91-4.